Characterizing the Dynamics of Solvated Disaccharides with in-Electrospray Ionization Hydrogen/Deuterium Exchange-Mass Spectrometry

Ana V. Quintero[1], O. Tara Liyanage[1,‡], H. Jamie Kim[1,†], Elyssia S. Gallagher[1,*]

[1]Department of Chemistry and Biochemistry, Baylor University, One Bear Place #97348, Waco, TX 76798, USA

*Corresponding Author:
Elyssia S. Gallagher
Department of Chemistry and Biochemistry, Baylor University, One Bear Place #97348, Waco, TX 76798, USA
Phone: (254) 710-2783
Email: elyssia_gallagher@baylor.edu

‡Current address:
Amgen Inc., Cambridge, Massachusetts 02141, USA

†Current address:
Division of Biology, Chemistry, and Material Science, Office of Science and Engineering Laboratories, Center for Devices and Radiological Health, U.S. Food and Drug Administration, 10903 New Hampshire Ave, Silver Spring, MD 20903, USA

Abstract

Carbohydrates have various biological functions that are based on their structures. However, the composition and the glycosidic-bond linkage and configuration of carbohydrates present challenges for their characterization. Furthermore, isomeric features contribute to the formation of intramolecular hydrogen bonds, which influence the flexibility and dynamics of carbohydrates. Hydrogen/deuterium exchange-mass spectrometry (HDX-MS) enables the analysis of protein dynamics by monitoring deuterium labeling after HDX for different lengths of time. In-electrospray ionization (in-ESI) HDX-MS has been used to rapidly label solvated carbohydrates with labeling occurring during desolvation of ESI droplets. Therefore, HDX-labeling times can be altered by changing the spray-solvent conductivity, which changes the initial size of ESI droplets and their resulting lifetimes. Here, we utilize in-ESI HDX-MS to characterize nine isomeric disaccharides with different monosaccharide compositions and glycosidic-bond linkages and configurations. We compared both the relative *D*-uptake of isomers at individual conductivities, or HDX-labeling times, and the trends associated with labeling at multiple conductivities. Interestingly, the relative *D*-uptake trends were correlated to isomeric features that affect disaccharide flexibility, including formation of intramolecular hydrogen bonds. Among the isomeric features studied, linkage was observed to have a significant influence on relative *D*-uptake with (1-3)-linked disaccharides having more change in relative *D*-uptake with changing conductivity compared to other linkages. Overall, this research illustrates how in-ESI HDX-MS can be applied to structurally characterize disaccharides with distinct isomeric features. Furthermore, this work shows that in-ESI HDX-MS can be used to monitor the dynamics of solvated molecules with rapidly exchanging functional groups.

Introduction

Carbohydrates, which have vital biological roles in cellular communication and metabolism,[1, 2] are composed of monosaccharides that are joined by glycosidic bonds**,** resulting in linkage and/or configurational isomers.[3] These structural characteristics contribute to the formation of biologically relevant, complex carbohydrates, such as human milk oligosaccharides (HMOs).[4] HMOs support the development of an infant's gut microbiome, providing beneficial bacteria for an infant's health, preventing viral infections, and enhancing cognitive development.[4] Because carbohydrate structures affect their biological functions, structural characterization is valuable; however, isomeric features make this challenging.

Hydrogen/deuterium exchange-mass spectrometry (HDX-MS) is commonly applied to the analysis of protein structures and dynamics;[5, 6] though, HDX-MS is also emerging as a valuable method to study carbohydrates.[7, 8] During HDX, labile hydrogen atoms attached to nitrogen, oxygen, and sulfur exchange rapidly with deuterium from deuterating reagents, such as deuterium oxide, deuterated ammonia, or deuterated methanol.[9] Exchange with deuterating reagents results in deuterium incorporation that can be quantified by measuring the mass difference between the undeuterated and deuterated species using MS.[10] Protein dynamics are monitored by measuring deuterium labeling at backbone amides after incubating the protein in D_2O-containing buffer for different lengths of time.[11] Carbohydrates cannot undergo deuterium labeling with traditional HDX-MS techniques due to the presence of rapidly exchanging hydroxyl groups.[12] Thus, in-electrospray ionization (ESI) HDX-MS introduces deuterating reagent to the analyte during the ESI process.[8, 13] Because evaporation of ESI droplets and exchange rates for hydroxyls occur on similar timescales of microseconds to milliseconds,[14] carbohydrates can be labeled by HDX during ESI.

Prior work has shown that carbohydrate-metal adducts experience minimal exchange in the gas phase.[8] Therefore, HDX-labeling times for in-ESI HDX can be modified by altering the desolvation time of the initial ESI droplets, e.g. by using different-sized theta-tip emitters[15] or by changing the conductivity of the spray-solvent.[16] ESI droplets with large diameters take more time to desolvate than smaller droplets; thus, HDX-labeling time increases as ESI droplet size increases.[7, 8, 15, 16] Scaling laws describe the relationship between the initial diameter of ESI droplets and the properties of electrosprayed solutions,[17, 18] including solution conductivity,[19] solvent composition,[20] flow rate,[21] the size of the electrospray emitter,[22] and the droplet charge-to-volume ratio.[23]

In-ESI HDX-MS was previously used to distinguish three trisaccharide isomers.[16] It was demonstrated that melezitose and isomaltotriose, trisaccharide isomers that differ in linkage and composition, could not be distinguished by monitoring HDX at only a single spray-solvent conductivity, or a single HDX-labeling time. Yet, labeling for different lengths of time, by changing the spray-solvent conductivity, allowed for melezitose, isomaltotriose, and maltotriose to be distinguished from each other.[16] We hypothesize that this difference in HDX labeling is due to differences in the solvated conformations and dynamics of these isomers.

The flexibility of carbohydrate structures is associated with their hydrogen-bonding networks, which include intramolecular hydrogen bonds between monosaccharide rings and intermolecular hydrogen bonds with solvent. Figure 1 shows the dihedral angles at the glycosidic bond (ϕ, ψ, and ω) between monosaccharides for three disaccharides: nigerose, maltose, and isomaltose. The dihedral angles influence the hydrogen-bonding networks and the overall, solvated structures of these disaccharides. Simulations have shown how the flexibility and entropy of oligosaccharides varies in relation to intramolecular hydrogen bonding.[24-28] Molecular dynamics studies of eight

disaccharides, composed of glucose, in water – kojibiose (α1-2), sophorose (β1-2), nigerose (α1-3), laminaribiose (β1-3), maltose (α1-4), cellobiose (β1-4), isomaltose (α1-6), and gentiobiose (β1-6) – showed that intramolecular hydrogen bonds formed for all disaccharides, except for the (1-6)-linked isomaltose and gentiobiose.[26] The lack of intramolecular hydrogen bonds in (1-6)-linked disaccharides (Figure 1C) resulted in highly flexible structures.[25, 26] Nigerose was shown to have intramolecular hydrogen bonds between H(O4′) and O2 as well as H(O2′) and O5[26] (dashed lines in Figure 1A) whereas maltose was shown to have intramolecular hydrogen bonds between H(O2) and O3′ in addition to H(O3′) and O2[25, 26, 29] (Figure 1B). Furthermore, simulations showed that the (1-6)-linked isomaltose formed more intermolecular hydrogen bonds with water compared to the (1-4)-linked maltose.[25]

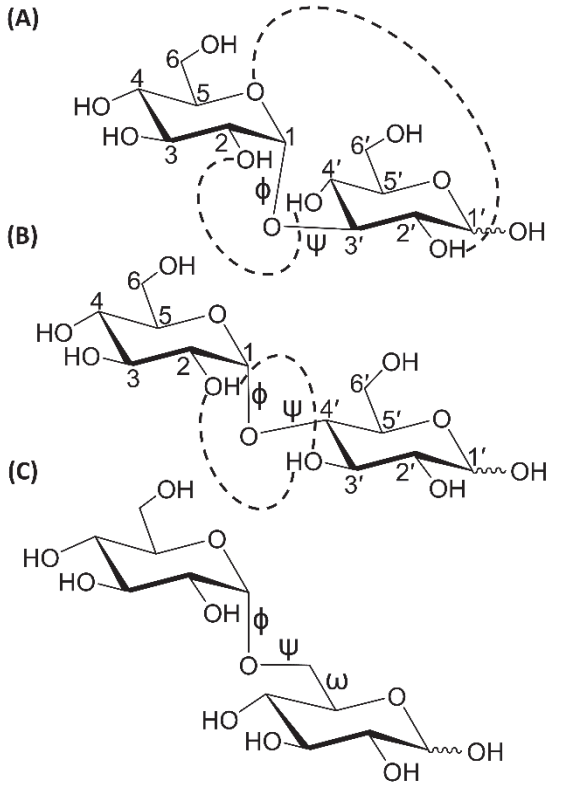

Figure 1. (A) Nigerose, **(B)** maltose, and **(C)** isomaltose with ϕ, ψ, and ω dihedral angles. Nonreducing (left) and reducing (right) monosaccharide units are denoted without and with primes, respectively. Intramolecular hydrogen bonds for **(A)** nigerose and **(B)** maltose are depicted with dashed lines and based on prior descriptions.[25-26, 29] **(C)** Compared to nigerose and maltose, isomaltose exhibits increased flexibility due to the additional dihedral angle, ω, and lack of intramolecular hydrogen bonds.

In this work, disaccharide isomers with differences in composition and glycosidic-bond linkage and configuration were investigated by in-ESI HDX-MS. Different spray-solvent conductivities were used to generate initial ESI droplets with different sizes, and thus different desolvation times. Consequently, different spray-solvent conductivities correlate to different HDX-labeling times, enabling differences in the dynamics of the disaccharides to be analyzed.

Here, we correlate differences in HDX labeling to isomeric features in disaccharides that have previously been related to intramolecular hydrogen bonding and carbohydrate flexibility. This work shows that in-ESI HDX can sample the dynamics of carbohydrates in solution, which may enhance our knowledge of the structure-function relationship for this class of biomolecules.

Experimental

Materials and Reagents

D-(+)-maltose monohydrate, D-(+)-cellobiose, melibiose, sodium chloride (NaCl), and Girard's reagent T were from Sigma Aldrich (St. Louis, MO). β-D-Gentiobiose, nigerose, and laminaribiose were from Biosynth International, Inc. (San Diego, CA). D-lactose was from BeanTown Chemical (Hudson, NH). Isomaltose and maltoheptaose were from Cayman Chemical (Ann Arbor, MI). Sophorose was from Neogen (Lansing, MI). All saccharides had a purity ≥95%, except for nigerose (≥93%) and maltoheptaose (≥80%). Deuterium oxide (D_2O, 99.96% purity) was from Cambridge Isotope Laboratories, Inc (Tewksbury, MA). Methanol and acetic acid were from Fisher Scientific International, Inc. (Pittsburgh, PA). All chemicals were used without further purification. Nanopure water was obtained from a Purelab Flex 3 water purification system (Elga, Veolia Environment S. A., Paris, France).

Internal Standard Preparation

Internal standards (IS) reduce systematic error, improving the repeatability of HDX-MS analyses.[16, 30-33] Therefore, an IS was included in all in-ESI HDX-MS experiments. Maltoheptaose was selected as the IS due to its structural similarity to the disaccharide analytes, which contain many rapidly exchanging hydroxyl groups. Maltoheptaose was derivatized and purified based on

previously published methods.[16, 32, 34] In short, an excess of Girard's reagent T was reacted with maltoheptaose for 3 h at 75 °C in 8.5:1.5 (v/v) methanol: acetic acid. Then, a nitrogen blowdown evaporator (Reacti-Therm module, Thermo-Fisher Scientific, Waltham, MA) was used to concentrate the sample followed by purification using PD MidiTrap G-10 columns (1 mL of sample per column) (Cytiva, Marlborough, MA) to remove excess Girard's reagent T. Eight 0.5-mL fractions were collected per column and analyzed using a LTQ Orbitrap Discovery MS (Thermo-Fisher Scientific, Waltham, MA). From the eight fractions, two consecutive 0.5-mL fractions were selected to be repurified based on these criteria: (1) derivatized maltoheptaose (1266 *m/z*) was observed between 70% to 100% relative abundance and (2) sodiated Girard's reagent T (644 *m/z*) was observed at 50% or less relative abundance. The two fractions that contained derivatized maltoheptaose were combined, repurified with PD MidiTrap G-10 columns to collect an additional set of eight 0.5-mL fractions, and analyzed. Purification was performed a second time to collect fractions that had increased concentration and purity of derivatized maltoheptaose, compared to Girard's reagent T. All fractions from the second round of purification that met the criteria stated above (1 and 2) were frozen at -80 °C for 48 h, lyophilized for 48 h, pooled, and reconstituted in methanol, resulting in a final stock concentration of 3.4 mM, which was spiked into all samples for analyses. The final IS concentration in all disaccharide samples was as low as possible to enable adequate signal for MS detection, while minimizing potential interactions between the IS and/or the disaccharides during in-ESI HDX.

Sample Preparation

Separate stock solutions of each disaccharide (0.1 M) and NaCl (0.2 M) were made in nanopure water. Each disaccharide (500 µM) was prepared with varying concentrations of NaCl (90 µM–

790 μM) in 99:1 (v/v) methanol: water, resulting in five solutions with different conductivities. A solution of 0.2 M NaCl, diluted in 99:1 (v/v) methanol: water, was used to modify the conductivities for each disaccharide solution and conductivities were measured with the Thermo Scientific Orion 013005MD DuraProbe 4-Electrode conductivity cell probe connected to the Orion Star A215 conductivity meter (Thermo-Fisher Scientific, Waltham, MA). For each disaccharide, 5 mL of the conductivity-measured solution was transferred to a centrifuge tube, spiked with 20 μL internal standard stock solution,[32, 34] and used for in-ESI HDX-MS analyses. Conductivities of each of these final solutions were measured with the Oakton 2-Cell conductivity probe connected to the Oakton CON 700 benchtop meter (Oakton Instruments, Vernon Hills, IL) and had conductivities of approximately (7, 34, 47, 59, and 83) μS/cm. All solutions were prepared fresh daily.

In-ESI HDX Experiments

A LTQ Orbitrap Discovery mass spectrometer with an Ion Max source was used to conduct in-ESI HDX experiments with a previously published method.[16] In brief, 200 μL of D_2O was placed on a metal plate to generate D_2O vapor inside the source. Acquisitions for deuterated disaccharides were collected for 5.0 min and spectra were averaged between 4.0–4.2 min, a timeframe that has been shown to yield a consistent partial pressure of D_2O vapor inside the ESI source.[8, 16] Because the partial pressure of the D_2O vapor is consistent at this acquisition time, the rate of D_2O vaporization is not changing, minimizing the effect of this rate constant on HDX. The source was evacuated for 2.0 min between each acquisition, preventing in-source accumulation of residual solvent vapor.[35] Between disaccharide solutions of different conductivities, the source was evacuated for 5.0 min. Acquisitions for undeuterated disaccharides did not utilize the D_2O droplet

on the plate and were collected for 5.0 min, with spectra averaged between 4.5–5.0 min. ESI source parameters consisted of sheath gas: 12 arb units, auxiliary gas: 0 arb units, sweep gas flow rate: 0 arb units, spray voltage: 3.50 kV, capillary temperature: 300 °C, capillary voltage: 40 V, and sample infusion flow rate: 20 μL/min.

Data Analysis

Weighted-average masses (*M*) of undeuterated and deuterated disaccharides were calculated using equation (1) based on the experimental mass-to-charge values (*m/z*), ion intensities (*I*), and the charge state of the analyte (*z*).

$$M = \left[\frac{\Sigma\,(m/z \times I)}{\Sigma I}\right] \times z \tag{1}$$

The average number of HDX, or *D*-uptake values, were determined by calculating the difference between the weighted-average mass of deuterated ($M_{\mathrm{Deuterated}}$) and undeuterated ($M_{\mathrm{Undeuterated}}$) disaccharides, as shown in equation (2)

$$D\text{-uptake} = M_{\mathrm{Deuterated}} - M_{\mathrm{Undeuterated}} \tag{2}$$

The IS, derivatized maltoheptaose, is under the same conditions as each disaccharide because it is present in every run. Therefore, the IS serves as a marker showing systematic variations in HDX as environmental conditions change between runs on different days.[16, 32] Therefore, we report relative *D*-uptake values, which are calculated using the ratio of *D*-uptake for the sodiated disaccharide to the *D*-uptake of the IS (equation 3).

$$\text{Relative } D\text{-uptake} = \frac{D\text{-uptake disaccharide}}{D\text{-uptake IS}} \tag{3}$$

Conductivity values, *D*-uptake values for the disaccharides and IS, and relative *D*-uptake values are presented as the average ± the standard error of the mean (SEM) for a minimum of three

replicates on a minimum of four days (Table S1). The term 'relative *D*-uptake value(s)' refers to the specific value at each conductivity, or HDX-labeling time (Table S1). In contrast, the term 'relative *D*-uptake trend' refers to the trendline, or slope, of the relative *D*-uptake values over a range of conductivities between 34 μS/cm and 83 μS/cm (Table S2 and Figure S1).

Grubb's tests were performed for relative *D*-uptake values collected for a single disaccharide at each conductivity to remove any outliers at the 95% confidence interval. Then, dual statistical tests, as proposed by Hageman and Weis for protein analyses to minimize overinterpreting HDX measurements, were applied.[36] Welch's *t* tests and confidence interval (CI) tests at the 95%, 99%, and 99.9% confidence level were utilized for statistical comparisons. When calculating confidence intervals, some comparisons had degrees of freedom between either 31-39, 41-49, or 51-61. To calculate confidence intervals at the 99.9% confidence level, *t* values for 30, 40, and 60 degrees of freedom, respectively, were used. Both statistical tests had to pass for relative *D*-uptake values to be considered statistically significant at the 95%, 99%, or 99.9% confidence level.

Results and Discussion

We chose isomeric disaccharides with multiple structural differences to sample the dynamics of carbohydrates. The chemical structures and associated symbol representations are shown in Figure 2. Though the majority of these disaccharides have glucose monosaccharides, two of the disaccharides contain galactose. The selected isomeric disaccharides also have differences in their glycosidic-bond linkage and configuration. Carbohydrate conformations are described by their glycosidic-bond dihedral angles – ϕ, ψ, and ω (Figure 1), which influence the formation and occurrence of hydrogen bonds, affecting the flexibility and dynamics of carbohydrates.[25, 26] When

disaccharide flexibility and dynamics are discussed herein, it relates to the formation and occurrence of intramolecular hydrogen bonds between the monosaccharide subunits.

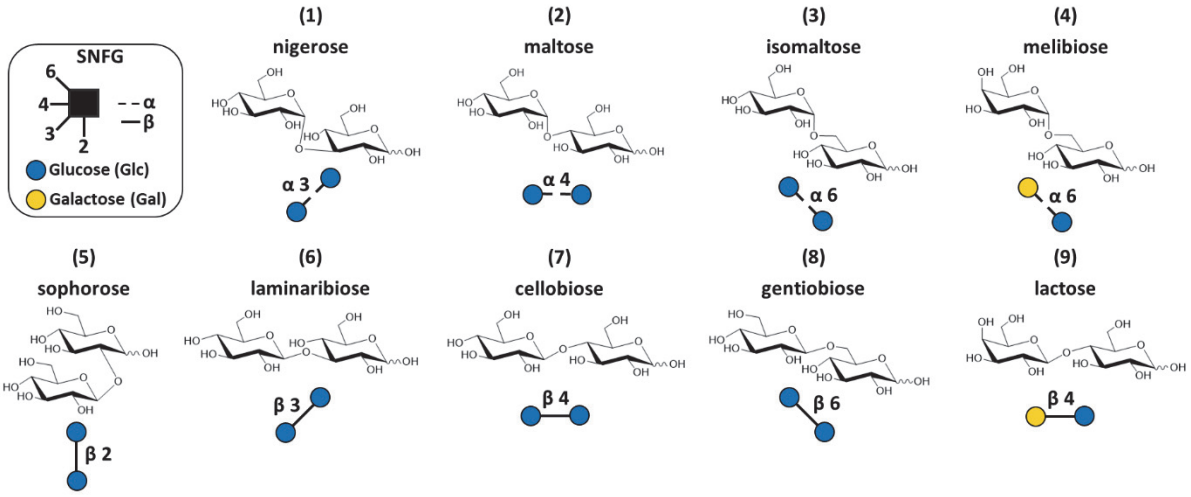

Figure 2. Disaccharide structures and corresponding pictorial representations, according to the symbol nomenclature for glycans (SNFG): **(1)** nigerose (Glc(α1-3)Glc), **(2)** maltose (Glc(α1-4)Glc), **(3)** isomaltose (Glc(α1-6)Glc), **(4)** melibiose (Gal(α1-6)Glc), **(5)** sophorose (Glc(β1-2)Glc), **(6)** laminaribiose (Glc(β1-3)Glc), **(7)** cellobiose (Glc(β1-4)Glc), **(8)** gentiobiose (Glc(β1-6)Glc), and **(9)** lactose (Gal(β1-4)Glc).

(1-3) linkage has a significant effect on the relative D-uptake of disaccharides

For the disaccharides, *D*-uptake values decrease with increasing spray-solvent conductivity (Table S1). This is expected because increasing conductivity results in formation of ESI droplets with decreasing size.[16, 17] ESI droplets that vary in size are expected to have different surface area-to-volume ratios and surface tensions, which could affect the permeability of D_2O vapor into the droplets.[37, 38] However, the *D*-uptake values in Table S1 illustrate a correlation between spray-solvent conductivity and the amount of HDX labeling. Thus, this data suggests that spray solvents with increasing conductivity yield smaller ESI droplets that desolvate faster, and have reduced labeling time for HDX, resulting in lower *D*-uptake. Figure S2 shows that *D*-uptake values vary between runs, which were collected over multiple months of experiments. Therefore, an IS was used and relative *D*-uptake values were reported, which improved measurement repeatability.[32]

Thus, relative *D*-uptake values are used to compare disaccharide isomers at multiple conductivities, or HDX-labeling times.

By using multiple spray-solvent conductivities, or sampling HDX at multiple timepoints, several α-linkage isomers could be distinguished from each other (Figure S3A). Three α-linkage isomers differ in the position of the glycosidic bond: with nigerose **(1)**, maltose **(2)**, and isomaltose **(3)** having (α1-3), (α1-4), and (α1-6) linkages, respectively (Figure 2). When comparing the relative *D*-uptake values for the α-linked disaccharides at each conductivity, the values for maltose and isomaltose were within measurement error (Figure 3A and Table S1). Whereas the relative *D*-uptake values for nigerose were distinguished from those for both maltose and isomaltose at all conductivities (Figures 3B, C and Table S1). Complete deuteration of the labile hydroxyls for the α-linkage isomers was not observed for any conductivity or HDX-labeling time due to back-exchange in the ESI source due to ambient humidity and/or residual solvent vapors.[35] Representative mass spectra for nigerose, maltose, and isomaltose at all conductivities are shown in Figure S4A-C.

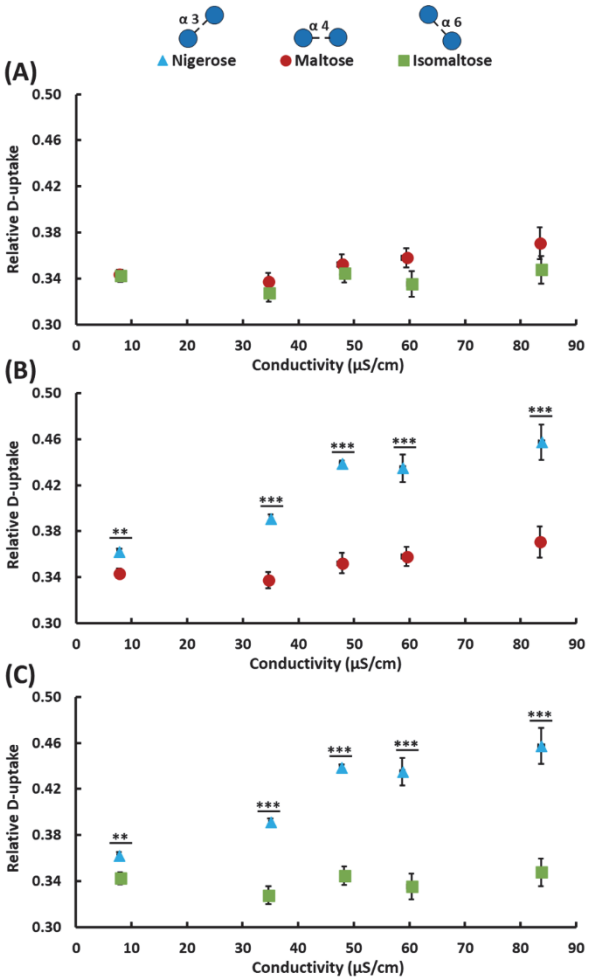

Figure 3. Scatter plots of relative *D*-uptake for α-linked disaccharide isomers (M) detected as $[M + Na]^+$. **(A)** Maltose (red circles) and isomaltose (green squares), **(B)** nigerose (light blue triangles) and maltose, and **(C)** nigerose and isomaltose. Data was collected over multiple days. Vertical error bars ($n \geq 15$) and horizontal error bars ($n = 16$) that cannot be observed are smaller than the data symbols. $^{**}p < 0.01$ and $^{***}p < 0.001$. Comparisons of relative *D*-uptake without * are within measurement error and do not show statistical differences.

The relative *D*-uptake values for nigerose, maltose, and isomaltose were similar to each other at the lowest conductivity, or longest HDX-labeling time, but extended over a wider range of values at the highest conductivity, or shortest HDX-labeling time (Figures 3, S3A and Table S1). The difference in the relative *D*-uptake values for conductivities between 34 μS/cm and 83 μS/cm, resulted in nigerose having a greater slope for the relative *D*-uptake trend ($m = 0.0012 \pm 0.0005$) compared to isomaltose ($m = 0.0003 \pm 0.0002$) (Table S2). Additionally, though maltose and isomaltose did not have differences in relative *D*-uptake at any single conductivity (Figure 3), their slopes differed ($m = 0.0006 \pm 0.0001$ for maltose), enabling these disaccharides to be distinguished. This data demonstrates the utility of sampling multiple HDX-labeling times to detect linkage differences between disaccharides.

The uncertainty of the relative *D*-uptake values increased as the spray-solvent conductivity increased (Table S1). We hypothesize that the change in uncertainty correlates to the ESI droplet sizes. The ESI droplets formed at the lowest conductivity are expected to be the largest in size, have the greatest volume of solvent, and have the longest HDX times compared to droplets formed from spray solvents with the highest conductivity. However, at a single conductivity, ESI is expected to produce a distribution of droplet sizes. Variations in ESI droplet size for small droplets formed at high conductivity may yield more significant percent differences in droplet volume, and thus, desolvation and HDX-labeling time compared to the larger droplets, resulting in greater uncertainty in the measurements.

A set of β-linked disaccharides was also analyzed by in-ESI HDX-MS and the relative *D*-uptake values were compared (Figures 4, S3B and Table S1). A β(1-2)-linked disaccharide was compared to the other β-linkage isomers. Sophorose (β1-2) **(5)** was distinguished from laminaribiose (β1-3) **(6)** at three conductivities, which correlate to three HDX-labeling times, while sophorose was distinguished from gentiobiose (β1-6) **(8)** at two conductivities (Figures 4A and 4C). Sophorose (β1-2) and cellobiose (β1-4) **(7)** were distinguished at only the lowest conductivity (Figure 4B), while gentiobiose (β1-6) was distinguished from cellobiose (β1-4) at only the highest conductivity (Figure 4F). Laminaribiose (β1-3) and cellobiose (β1-4) were distinguished at three conductivities (Figure 4D), whereas laminaribiose (β1-3) and gentiobiose (β1-6) were distinguished at all conductivities, except for at the lowest conductivity (Figure 4E). Representative mass spectra for all β-linkage isomers at all conductivities are shown in Figure S4E-H. Sampling HDX at multiple labeling times resulted in more distinction between the β-linked disaccharides. Similar to nigerose, the (α1-3)-linked disaccharide, the (β1-3)-linked disaccharide, laminaribiose, was also distinguished at more conductivities, or HDX-labeling times, compared to the other β-linked disaccharides.

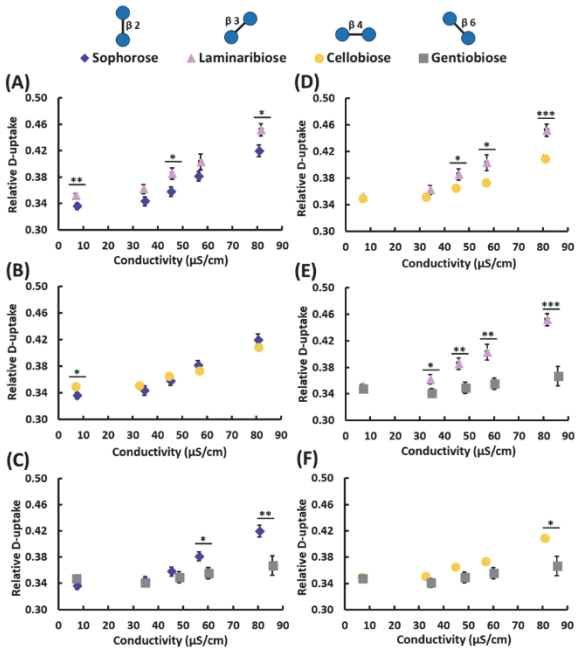

Figure 4. Scatter plots of relative *D*-uptake for β-linked disaccharide isomers (M) detected as $[M + Na]^+$. **(A)** Sophorose (dark blue diamonds) and laminaribiose (light purple triangles), **(B)** sophorose and cellobiose (yellow circles), **(C)** sophorose and gentiobiose (grey squares), **(D)** laminaribiose and cellobiose, **(E)** laminaribiose and gentiobiose, and **(F)** cellobiose and gentiobiose. Data was collected over multiple days. Vertical error bars ($n \geq 19$) and horizontal error bars ($n \geq 20$) that cannot be observed are smaller than the data symbols. $*p < 0.05$, $**p < 0.01$, and $***p < 0.001$. Comparisons of relative *D*-uptake without * are within measurement error and do not show statistical differences.

Similar relative *D*-uptake trends were observed between the α- and β-linkage isomers

(Figures 3, 4, and S3A-B). Comparable to the α-linkage isomers, the relative *D*-uptake values for the β-linkage isomers were within a narrow range of values at the lowest conductivity, or longest HDX labeling time, and exhibited a wider range of values at the highest conductivity or shortest HDX labeling time. Additionally, similar to nigerose (α1-3) **(1)** and isomaltose (α1-6) **(3)**, the β(1-3)-linked laminaribiose **(6)** and β(1-6)-linked gentiobiose **(8)** had the highest (m = 0.0019 ± 0.0001) and lowest (m = 0.00050 ± 0.00003) slopes, respectively, for the β-linked disaccharides (Table S2).

The relative *D*-uptake trends for the α- and β-linkage isomers observed here revealed similarities to past computational work.[26, 39] Nigerose (α1-3) was reported to form more intramolecular hydrogen bonds than maltose (α1-4), resulting in structures that were less flexible and less dynamic.[26] Conversely, isomaltose (α1-6) and gentiobiose (β1-6) do not form intramolecular hydrogen bonds, due to the (1-6) linkage, suggesting that these structures would be highly dynamic and flexible.[26] We hypothesize that the relative *D*-uptake trends correlate with the dynamics and flexibility of these carbohydrates. For example, isomaltose and gentiobiose with (1-6)-linkages are the most flexible disaccharides,[39] which we hypothesize correlates to the lowest slopes for the relative *D*-uptake trends (m = 0.0003 ± 0.0002 and 0.00050 ± 0.00003, respectively). For the α-linkage isomers, nigerose (m = 0.0012 ± 0.0005), maltose (m = 0.0006 ± 0.0001), and isomaltose (m = 0.0003 ± 0.0002) (Table S2), have increasing flexibility based on their respective linkages and decreasing slopes when comparing their relative *D*-uptake trends.

We generally observe an increase (positive slope) in relative *D*-uptake with increasing conductivity for α- and β-linkage isomers (Table S2). The lifetimes of hydrogen bonds (sub-ps)[25] are much shorter than the time for the HDX reactions performed during ESI (μs–ms).[14] In solution, hydrogen bonds are at an equilibrium where they constantly form and break. HDX occurs at sites

where intramolecular hydrogen bonds are not present.[7, 9] Spray solvents with high conductivity produce small ESI droplets, and have short times for HDX labeling, producing a wide range of relative *D*-uptake values for both α- and β-linkage isomers. We hypothesize that this range of relative *D*-uptake values is because of the specific linkages that contribute to differences in the occurrence and formation of intramolecular hydrogen bonds. In these small droplets, rapid labeling occurs at sites that do not participate in intramolecular hydrogen bonds; therefore, differences in the dynamics of each linkage isomer are associated with differences in HDX. In contrast, at low conductivities, relative *D*-uptake values tend to be similar for the α- and β-linkage isomers. Because this conductivity yields the largest ESI droplets, we hypothesize that the labeling time is sufficient that even disaccharides that form more intramolecular hydrogen bonds have equilibrated to the "broken" state of the hydrogen bonds, enabling HDX and resulting in little distinction in relative *D*-uptake among the isomers. Overall, these results demonstrate that variations in disaccharide linkage yield different relative *D*-uptake trends and we observe a correlation based on the intramolecular hydrogen bonding and the associated flexibility of these disaccharides.

The IS, derivatized maltoheptaose, is a carbohydrate with (1-4) linkages. (1-4)-linked disaccharides have infrequent intramolecular hydrogen bonds, with more intramolecular hydrogen bonds compared to (1-6)-linked disaccharides but fewer intramolecular hydrogen bonds than (1-3)-linked disaccharides.[25, 26] Therefore, we hypothesize that the flexibility of the IS will be between that of (1-3)- and (1-6)-linked oligosaccharides, though the longer chain may enable additional intramolecular hydrogen bonds in the IS compared to the disaccharides, affecting the flexibility of the IS. The reported relative *D*-uptake values are therefore influenced by the flexibility and associated *D*-uptake for each disaccharide and the IS. Thus, rather than seeing more rapid *D*-uptake for the more flexible, (1-6)-linked disaccharides, the trends for relative *D*-uptake account for the

flexibility and dynamics of both the disaccharide and the IS. Because the IS is the same for each run, the observed trends in relative *D*-uptake highlight differences in the disaccharide dynamics.

In our previous study, trisaccharide isomers, maltotriose (α1-4) and isomaltotriose (α1-6), were distinguished at all reported conductivities.[16] We hypothesize that the additional monosaccharide unit and the multiple isomeric features of the trisaccharides, affect the formation of intramolecular hydrogen bonds and is the primary reason for differences in the relative *D*-uptake trends compared to the disaccharides analyzed here.

Differences in relative D-uptake values are observed for (1-3)-linked configurational isomers

The configuration for carbohydrate linkages is challenging to obtain with MS-based methods.[40] Tandem MS cannot distinguish configurational isomers.[40] Ion mobility (IM)-MS can utilize different metal-ion adducts to improve the separation of carbohydrate isomers;[41] yet, the ideal metal for separating a particular set of isomers is challenging to predict.[41, 42] Additionally, tandem MS and IM-MS characterize gas-phase structures of carbohydrates, which vary from the solvated, dynamic conformations that exist in biological systems.[43] Consequently, we used in-ESI HDX-MS to study three pairs of configurational isomeric disaccharides (Figures 5, S3C). The (1-3)-linked isomer pair, nigerose (α1-3) **(1)** and laminaribiose (β1-3) **(6),** were distinguished at three conductivities, which correlate to three HDX-labeling times (Figure 5A), whereas the (1-4)-linked configurational isomeric pair, maltose (α1-4) **(2)** and cellobiose (β1-4) **(7)** were distinguished at the highest conductivity (Figure 5B). In contrast, the (1-6)-linked configurational isomeric pair, isomaltose (α1-6) **(3)** and gentiobiose (β1-6) **(8)**, were not distinguished at any conductivities (Figure 5C). Although the (1-3)- and (1-4)-linked configurational isomeric pairs could be

distinguished, the glycosidic-bond linkage contributed to the observed slopes for the relative *D*-uptake trends for each set of configurational isomers. We hypothesize that the slopes for the (1-6)-linked configurational isomeric pair, isomaltose and gentiobiose, with the lowest relative *D*-uptake trends, correlate to their greater flexibilities, compared to the (1-3)- and (1-4)-linked configurational isomeric pairs (Table S2). Expanding on this, we hypothesize that the (1-3)-linked configurational isomeric pair, nigerose and laminaribiose, which have the highest slopes for the relative *D*-uptake trends, correspond to structures with low flexibility (Table S2).

Past work has described how the configuration of the glycosidic bond affects the flexibility of (1-4)- and (1-6)-linked disaccharides, including maltose (α1-4), cellobiose (β1-4), isomaltose (α1-6), and gentiobiose (β1-6).[39] Generally, the β-linked configurational isomers were revealed to be more flexible compared to their α-linked stereoisomers.[39] However, cellobiose (β1-4) was computationally observed to form more intramolecular hydrogen bonds than maltose

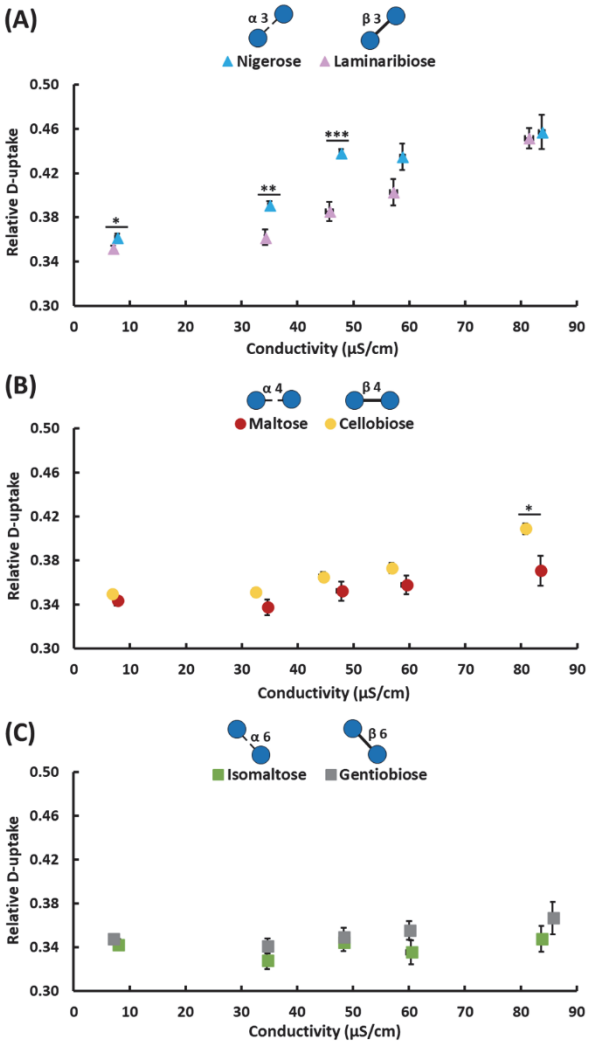

Figure 5. Scatter plots of relative *D*-uptake for configurational disaccharide isomers (M) detected as $[M + Na]^+$. **(A)** Nigerose (light blue triangles) and laminaribiose (light purple triangles), **(B)** cellobiose (yellow circles) and maltose (red circles), and **(C)** isomaltose (green squares) and gentiobiose (grey squares). Data collected over multiple days. Vertical error bars ($n \geq 15$) and horizontal error bars ($n \geq 16$) that cannot be observed are smaller than the data symbols. $*p < 0.05$, $**p < 0.01$, and $***p < 0.001$. Comparisons of relative *D*-uptake without * are within measurement error and do not show statistical differences.

(α1-4), which would be expected to decrease the flexibility of cellobiose.[26] Yet, experimental measurements showed that cellobiose had more conformational entropy than maltose.[39] Our data shows that cellobiose had a greater slope than maltose, which suggests a less flexible structure compared to maltose (Figure 5B and Table S2). Overall, these results suggest that differences in relative *D*-uptake trends result from not only the linkage, but also from differences in the glycosidic-bond configuration.

Disaccharides containing both galactose and glucose exhibit greater differences in relative D-uptake than glucose-based disaccharides

Lactose, which is composed of glucose and galactose, is a core constituent of HMOs, which can be extended at the galactose monosaccharide to form diverse structures.[4] Melibiose, which is also composed of glucose and galactose, also has roles in health.[44] Hence, we used in-ESI HDX-MS to investigate two pairs of compositional isomers, containing either glucose and galactose or only glucose – the β(1-4)-linked pair: cellobiose **(7)** and lactose **(9)**, and the α(1-6)-linked pair: isomaltose **(3)** and melibiose **(4)** (Figure 2). Representative mass spectra for melibiose and lactose at all conductivities are shown in Figure S4D and S4I. Relative *D*-uptake values were statistically different when comparing lactose and cellobiose at all conductivities except for 58 μS/cm (Figure 6A). Relative *D*-uptake values were statistically different for melibiose and isomaltose at all conductivities except for 48 μS/cm (Figure 6B).

Expanding on the prior discussion, (1-6) linkages in carbohydrates result in highly flexible structures compared to carbohydrates with (1-4) linkages, which have infrequent intramolecular hydrogen bonds.[25, 26] Moreover, (1-6)-linked configurational isomers were not distinguished at any conductivities, or HDX labeling times (Figure 5). When comparing disaccharides that are composed of glucose and galactose versus only glucose, distinctions were observed as a result of both the glycosidic bond linkage and the presence of galactose. These compositional isomeric pairs have the same glycosidic-bond linkage and configuration, with their respective linkage – (1-4) and (1-6) – contributing the most to the observed slope of the relative *D*-uptake trends. However, the monosaccharide units, and therefore the orientation of the carbon-4 hydroxyl on the nonreducing monosaccharide, differ between each pair of isomers, resulting in distinct differences between the relative *D*-uptake trends (Figure 6 and Table S2).

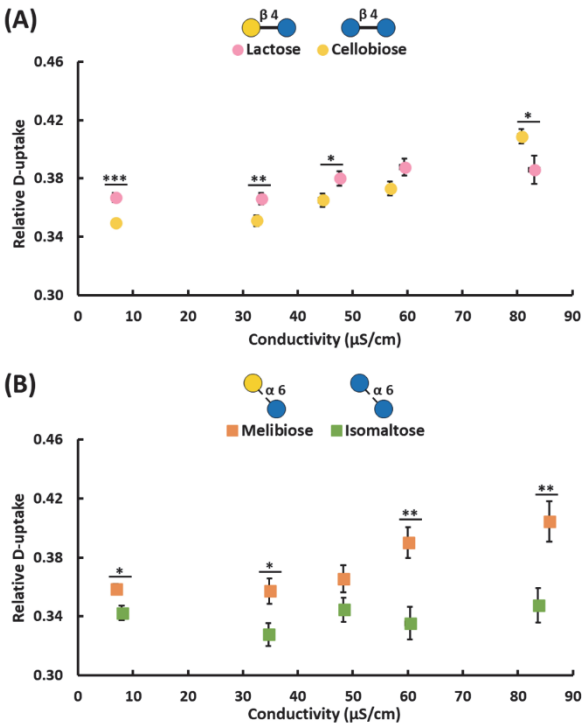

Figure 6. Scatter plots of relative *D*-uptake for compositional isomers (M) detected as $[M + Na]^+$. **(A)** Lactose (pink circles) and cellobiose (yellow circles) and **(B)** melibiose (orange squares) and isomaltose (green squares). Data was collected on multiple days. Vertical error bars ($n \geq 24$ for **(A)** and $n \geq 16$ for **(B)**) and horizontal error bars ($n \geq 16$) that cannot be observed are smaller than the data symbols. $*p < 0.05$, $**p < 0.01$, and $***p < 0.001$. Comparisons of relative *D*-uptake without * are within measurement error and do not show statistical differences.

Though we focus most of our discussion on comparing disaccharides with a single difference in isomeric features, multiple isomeric features can exist in carbohydrates, affecting their functions in biological systems.[1] Therefore, comparisons were made between disaccharides containing multiple differences in isomeric features to determine how relative *D*-uptake trends were affected

(see Supporting Information for additional details). As previously observed (Figures 3 and 4), linkage had a significant effect on the distinction of disaccharide isomers. When comparing additional disaccharides that differ in both linkage and composition, isomers could be distinguished at all but one conductivity (Figure S5B). Moreover, although (1-6)-linked configurational isomers were not distinguished previously (Figure 5C), disaccharides with differences in both composition and configuration of the glycosidic bond could be distinguished based on relative *D*-uptake values (Figures S5A, C). Because nigerose was distinct in that it could be distinguished from all other α-linkage isomers and from laminaribiose – its (1-3)-linked configurational isomer – at multiple conductivities, the relative *D*-uptake of nigerose was compared to that of disaccharides with a combination of isomeric features. The (1-3) linkage in nigerose was observed to have a significant impact on the relative *D*-uptake values when compared to disaccharides with a combination of isomeric features (Figures S5D-H), indicating that the (1-3) linkage in nigerose greatly influences the intramolecular hydrogen bonding, and thus its dynamics. Overall, these results show that disaccharides with defined isomeric features can be distinguished at multiple conductivities, which can be correlated to HDX labeling times.

Conclusions

Here, for the first time, we have shown that in-ESI HDX-MS can be used to characterize the solvated dynamics of disaccharides that differ in composition as well as glycosidic-bond linkage and configuration. The relative *D*-uptake trends observed herein correlate to the dynamics of the disaccharides, which we attribute to their isomeric features influencing intramolecular hydrogen bonding and the flexibility of the carbohydrates. The configuration of the glycosidic bond was observed to have a minimal influence on the observed relative *D*-uptake of disaccharide isomers,

while linkage and composition had greater effects on relative *D*-uptake, enabling more disaccharides to be distinguished. The data presented here correlates to past computational work for both α- and β-linkage isomers, suggesting that the solution-phase dynamics of disaccharides enable their differentiation by in-ESI HDX-MS. Although some of the linkages discussed herein are present in biological glycans and the presented results may provide insight into the structural dynamics of these glycans, we hypothesize that the relative *D*-uptake trends will differ in more complex glycans. The presence of monosaccharides with different types of exchangeable functional groups and their associated effects on intramolecular interactions that alter the dynamics of the glycans would also influence the relative *D*-uptake trends. Overall, this work shows that using rapid HDX to monitor labeling at multiple conductivities, or times, provides insight into the dynamics of solvated carbohydrates, which is crucial in understanding the relationship between their structural and functional properties, including those associated with molecular recognition.

Supporting Information

Relative *D*-uptake values for each disaccharide at each conductivity; slopes and R^2 values associated with linear fits for each disaccharide; scatter plots of relative *D*-uptake versus spray-solution conductivity for each disaccharide; plots of *D*-uptake and relative *D*-uptake for replicate runs; representative mass spectra; and additional comparisons of relative *D*-uptake for disaccharides with different isomeric features.

Acknowledgements

A.V.Q. was supported by the National Science Foundation (CHE-1945078). O.T.L. and H.J.K. were supported by the Welch Foundation (AA-1899). The authors would like to thank the Baylor University Mass Spectrometry Center and Molecular Biosciences Center.

Conflict of Interest Disclosure

The authors declare no competing financial interest.

References

(1) Gagneux, P.; Hennet, T.; Varki, A. Biological Functions of Glycans. In *Essentials of Glycobiology [Internet]*, 4th ed.; Cold Spring Harbor Laboratory Press: New York, 2022; pp 79-92.
(2) Dwek, R. A. Glycobiology: Toward Understanding the Function of Sugars. *Chem. Rev.* **1996**, *96* (2), 683-720. DOI: 10.1021/cr940283b.
(3) Seeberger, P. H. Monosaccharide Diversity. In *Essentials of Glycobiology [Internet]*, 4th ed.; Cold Spring Harbor Laboratory Press: New York, 2022; pp 21-32.
(4) Bode, L. Human milk oligosaccharides: Every baby needs a sugar mama. *Glycobiology* **2012**, *22* (9), 1147-1162. DOI: 10.1093/glycob/cws074.
(5) Engen, J. R. Analysis of Protein Conformation and Dynamics by Hydrogen/Deuterium Exchange MS. *Anal. Chem.* **2009**, *81* (19), 7870-7875. DOI: 10.1021/ac901154s.
(6) Konermann, L.; Pan, J.; Liu, Y.-H. Hydrogen exchange mass spectrometry for studying protein structure and dynamics. *Chem. Soc. Rev.* **2011**, *40* (3), 1224-1234. DOI: 10.1039/C0CS00113A.
(7) Hatvany, J. B.; Gallagher, E. S. Hydrogen/deuterium exchange for the analysis of carbohydrates. *Carbohydr. Res.* **2023**, *530*, 108859. DOI: 10.1016/j.carres.2023.108859.
(8) Liyanage, O. T.; Brantley, M. R.; Calixte, E. I.; Solouki, T.; Shuford, K. L.; Gallagher, E. S. Characterization of Electrospray Ionization (ESI) Parameters on In-ESI Hydrogen/Deuterium Exchange of Carbohydrate-Metal Ion Adducts. *J. Am. Soc. Mass Spectrom.* **2019**, *30* (2), 235-247. DOI: 10.1007/s13361-018-2080-1.
(9) Englander, S. W. Hydrogen exchange and mass spectrometry: A historical perspective. *J. Am. Soc. Mass Spectrom.* **2006**, *17* (11), 1481-1489. DOI: 10.1016/j.jasms.2006.06.006.
(10) Oganesyan, I.; Lento, C.; Wilson, D. J. Contemporary hydrogen deuterium exchange mass spectrometry. *Methods* **2018**, *144*, 27-42. DOI: 10.1016/j.ymeth.2018.04.023.
(11) James, E. I.; Murphree, T. A.; Vorauer, C.; Engen, J. R.; Guttman, M. Advances in Hydrogen/Deuterium Exchange Mass Spectrometry and the Pursuit of Challenging Biological Systems. *Chem. Rev.* **2022**, *122* (8), 7562-7623. DOI: 10.1021/acs.chemrev.1c00279.
(12) Guttman, M.; Scian, M.; Lee, K. K. Tracking Hydrogen/Deuterium Exchange at Glycan Sites in Glycoproteins by Mass Spectrometry. *Anal. Chem.* **2011**, *83* (19), 7492-7499. DOI: 10.1021/ac201729v.
(13) Kostyukevich, Y.; Kononikhin, A.; Popov, I.; Nikolaev, E. In-ESI Source Hydrogen/Deuterium Exchange of Carbohydrate Ions. *Anal. Chem.* **2014**, *86* (5), 2595-2600. DOI: 10.1021/ac4038202.
(14) Tittebrandt, S.; Edelson-Averbukh, M.; Spengler, B.; Lehmann, W. D. ESI Hydrogen/Deuterium Exchange Can Count Chemical Forms of Heteroatom-Bound Hydrogen. *Angew. Chem. Int. Ed.* **2013**, *52* (34), 8973-8975. DOI: 10.1002/anie.201304249.

(15) Kim, H. J.; Gallagher, E. S. Achieving multiple hydrogen/deuterium exchange timepoints of carbohydrate hydroxyls using theta-electrospray emitters. *Analyst* **2020**, *145* (8), 3056-3063. DOI: 10.1039/D0AN00135J.
(16) Liyanage, O. T.; Quintero, A. V.; Hatvany, J. B.; Gallagher, E. S. Distinguishing Carbohydrate Isomers with Rapid Hydrogen/Deuterium Exchange-Mass Spectrometry. *J. Am. Soc. Mass Spectrom.* **2021**, *32* (1), 152-156. DOI: 10.1021/jasms.0c00314.
(17) Fernández de la Mora, J. On the Outcome of the Coulombic Fission of a Charged Isolated Drop. *J. Colloid Interface Sci.* **1996**, *178* (1), 209-218. DOI: 10.1006/jcis.1996.0109.
(18) Gañán-Calvo, A. M.; Dávila, J.; Barrero, A. Current and droplet size in the electrospraying of liquids. Scaling laws. *J. Aerosol Sci.* **1997**, *28* (2), 249-275. DOI: 10.1016/S0021-8502(96)00433-8.
(19) Olumee, Z.; Callahan, J. H.; Vertes, A. Droplet Dynamics Changes in Electrostatic Sprays of Methanol−Water Mixtures. *J. Phys. Chem. A* **1998**, *102* (46), 9154-9160. DOI: 10.1021/jp982027z.
(20) Smith, J. N.; Flagan, R. C.; Beauchamp, J. L. Droplet Evaporation and Discharge Dynamics in Electrospray Ionization. *J. Phys. Chem. A* **2002**, *106* (42), 9957-9967. DOI: 10.1021/jp025723e.
(21) Schmidt, A.; Karas, M.; Dülcks, T. Effect of different solution flow rates on analyte ion signals in nano-ESI MS, or: when does ESI turn into nano-ESI? *J. Am. Soc. Mass Spectrom.* **2003**, *14* (5), 492-500. DOI: 10.1016/S1044-0305(03)00128-4.
(22) Mortensen, D. N.; Williams, E. R. Theta-Glass Capillaries in Electrospray Ionization: Rapid Mixing and Short Droplet Lifetimes. *Anal. Chem.* **2014**, *86* (18), 9315-9321. DOI: 10.1021/ac502545r.
(23) Gomez, A.; Tang, K. Charge and fission of droplets in electrostatic sprays. *Phys. Fluids* **1994**, *6* (1), 404-414. DOI: 10.1063/1.868037 (acccessed 5/3/2024).
(24) Stortz, C. A. Disaccharide conformational maps: how adiabatic is an adiabatic map? *Carbohydr. Res.* **1999**, *322* (1), 77-86. DOI: 10.1016/S0008-6215(99)00207-4.
(25) Best, R. B.; Jackson, G. E.; Naidoo, K. J. Molecular Dynamics and NMR Study of the α(1→4) and α(1→6) Glycosidic Linkages: Maltose and Isomaltose. *J. Phys. Chem. B* **2001**, *105* (20), 4742-4751. DOI: 10.1021/jp0040704.
(26) Pereira, C. S.; Kony, D.; Baron, R.; Müller, M.; van Gunsteren, W. F.; Hünenberger, P. H. Conformational and Dynamical Properties of Disaccharides in Water: a Molecular Dynamics Study. *Biophys. J.* **2006**, *90* (12), 4337-4344. DOI: 10.1529/biophysj.106.081539.
(27) Calixte, E. I.; Liyanage, O. T.; Kim, H. J.; Ziperman, E. D.; Pearson, A. J.; Gallagher, E. S. Release of Carbohydrate–Metal Adducts from Electrospray Droplets: Insight into Glycan Ionization by Electrospray. *J. Phys. Chem. B* **2020**, *124* (3), 479-486. DOI: 10.1021/acs.jpcb.9b10369.
(28) Calixte, E. I.; Liyanage, O. T.; Gass, D. T.; Gallagher, E. S. Formation of Carbohydrate–Metal Adducts from Solvent Mixtures during Electrospray: A Molecular Dynamics and ESI-MS Study. *J. Am. Soc. Mass Spectrom.* **2021**, *32* (12), 2738-2745. DOI: 10.1021/jasms.1c00179.
(29) Dowd, M. K.; Zeng, J.; French, A. D.; Reilly, P. J. Conformational analysis of the anomeric forms of kojibiose, nigerose, and maltose using MM3. *Carbohydr. Res.* **1992**, *230* (2), 223-244. DOI: 10.1016/0008-6215(92)84035-Q.
(30) Zhang, Z.; Zhang, A.; Xiao, G. Improved Protein Hydrogen/Deuterium Exchange Mass Spectrometry Platform with Fully Automated Data Processing. *Anal. Chem.* **2012**, *84* (11), 4942-4949. DOI: 10.1021/ac300535r.
(31) Uppal, S. S.; Beasley, S. E.; Scian, M.; Guttman, M. Gas-Phase Hydrogen/Deuterium Exchange for Distinguishing Isomeric Carbohydrate Ions. *Anal. Chem.* **2017**, *89* (8), 4737-4742. DOI: 10.1021/acs.analchem.7b00683.
(32) Liyanage, O. T.; Seneviratne, C. A.; Gallagher, E. S. Applying an Internal Standard to Improve the Repeatability of In-electrospray H/D Exchange of Carbohydrate-Metal Adducts. *J. Am. Soc. Mass Spectrom.* **2019**, *30* (8), 1368-1372. DOI: 10.1007/s13361-019-02153-2.

(33) Murphree, T. A.; Vorauer, C.; Brzoska, M.; Guttman, M. Imidazolium Compounds as Internal Exchange Reporters for Hydrogen/Deuterium Exchange by Mass Spectrometry. *Anal. Chem.* **2020**, *92* (14), 9830-9837. DOI: 10.1021/acs.analchem.0c01328.
(34) Naven, T. J. P.; Harvey, D. J. Cationic Derivatization of Oligosaccharides with Girard's T Reagent for Improved Performance in Matrix-assisted Laser Desorption/Ionization and Electrospray Mass Spectrometry. *Rapid Commun. Mass Spectrom.* **1996**, *10* (7), 829-834. DOI: 10.1002/(SICI)1097-0231(199605)10:7<829::AID-RCM572>3.0.CO;2-Y.
(35) Kim, H. J.; Liyanage, O. T.; Mulenos, M. R.; Gallagher, E. S. Mass Spectral Detection of Forward- and Reverse-Hydrogen/Deuterium Exchange Resulting from Residual Solvent Vapors in Electrospray Sources. *J. Am. Soc. Mass Spectrom.* **2018**, *29* (10), 2030-2040. DOI: 10.1007/s13361-018-2019-6.
(36) Hageman, T. S.; Weis, D. D. Reliable Identification of Significant Differences in Differential Hydrogen Exchange-Mass Spectrometry Measurements Using a Hybrid Significance Testing Approach. *Anal. Chem.* **2019**, *91* (13), 8008-8016. DOI: 10.1021/acs.analchem.9b01325.
(37) Tolman, R. C. The Effect of Droplet Size on Surface Tension. *J. Chem. Phys.* **1949**, *17* (3), 333-337. DOI: 10.1063/1.1747247 (acccessed 5/21/2024).
(38) Uhlig, H. H. The Solubilities of Gases and Surface Tension. *J. Phys. Chem.* **1937**, *41* (9), 1215-1226. DOI: 10.1021/j150387a007.
(39) Striegel, A. M. Anomeric Configuration, Glycosidic Linkage, and the Solution Conformational Entropy of O-Linked Disaccharides. *J. Am. Chem. Soc.* **2003**, *125* (14), 4146-4148. DOI: 10.1021/ja0214173.
(40) Gray, C. J.; Migas, L. G.; Barran, P. E.; Pagel, K.; Seeberger, P. H.; Eyers, C. E.; Boons, G.-J.; Pohl, N. L. B.; Compagnon, I.; Widmalm, G.; Flitsch, S. L. Advancing Solutions to the Carbohydrate Sequencing Challenge. *J. Am. Chem. Soc.* **2019**, *141* (37), 14463-14479. DOI: 10.1021/jacs.9b06406.
(41) Gass, D. T.; Quintero, A. V.; Hatvany, J. B.; Gallagher, E. S. Metal adduction in mass spectrometric analyses of carbohydrates and glycoconjugates. *Mass Spectrom. Rev.* **2022**, e21801. DOI: 10.1002/mas.21801.
(42) Huang, Y.; Dodds, E. D. Ion Mobility Studies of Carbohydrates as Group I Adducts: Isomer Specific Collisional Cross Section Dependence on Metal Ion Radius. *Anal. Chem.* **2013**, *85* (20), 9728-9735. DOI: 10.1021/ac402133f.
(43) Ma, X. Recent Advances in Mass Spectrometry-Based Structural Elucidation Techniques. *Molecules* **2022**, *27* (19), 6466.
(44) Tanaka, S.; Shinoki, A.; Hara, H. Melibiose, a Nondigestible Disaccharide, Promotes Absorption of Quercetin Glycosides in Rat Small Intestine. *J. Agric. Food Chem.* **2016**, *64* (49), 9335-9341. DOI: 10.1021/acs.jafc.6b03714.

For Table of Contents Only